

Heme oxygenase-1 deficiency presenting with interstitial lung disease and hemophagocytic flares

Alice S. Chau

Seattle Children's Research Institute

Bonnie L. Cole

Seattle Children's Hospital

Jason S. Debley

Seattle Children's Research Institute

Kabita Nanda

Seattle Children's Hospital

Aaron B.I. Rosen

Seattle Children's Research Institute

Michael J. Bamshad

Seattle Children's Hospital

Deborah A. Nickerson

University of Washington

Troy R. Torgerson

Seattle Children's Research Institute

Eric J. Allenspach (✉ eric.allenspach@seattlechildrens.org)

University of Washington <https://orcid.org/0000-0001-7346-5835>

Research

Keywords: HMOX1, heme oxygenase-1, HO-1, NSIP, systemic juvenile idiopathic arthritis, macrophage activation syndrome, asplenia, hemophagocytosis lymphohistiocytosis, vasculitis

Posted Date: February 28th, 2020

DOI: <https://doi.org/10.21203/rs.3.rs-15456/v1>

License:  This work is licensed under a Creative Commons Attribution 4.0 International License.

[Read Full License](#)

Version of Record: A version of this preprint was published at Pediatric Rheumatology on October 16th, 2020. See the published version at <https://doi.org/10.1186/s12969-020-00474-1>.

Abstract

Background Heme oxygenase-1 (HMOX1) catalyzes the metabolism of heme into carbon monoxide, ferrous iron, and biliverdin. Through biliverdin reductase, biliverdin becomes bilirubin. HMOX1 -deficiency is an exceedingly rare autosomal recessive disorder with hallmark features of direct antibody negative hemolytic anemia with normal bilirubin, hyperinflammation and features indicating hemophagocytosis lymphohistiocytosis. Clinical findings have included asplenia, nephritis, hepatitis, and evidence of vasculitis. Pulmonary features and evaluation of the immune response have been limited.

Results Here, we present the fifth reported case in literature of a young boy who remarkably also presented with chronic respiratory failure due to nonspecific interstitial pneumonia in addition to infection-triggered recurrent hyperinflammatory flares notable for hemolysis without hyperbilirubinemia, immunodeficiency, hepatomegaly with mild transaminitis, asplenia, leukocytosis, thrombocytosis, joint pain and features of macrophage activation with negative autoimmune serologies. Lung biopsy revealed cholesterol granulomas. He was found post-mortem by whole exome sequencing to have a compound heterozygous paternal frame shift a paternal frame shift HMOX1 c.264delCTGG (p.L89Sfs*24) and maternal splice donor HMOX1 (c.636+2 T>A) consistent with HMOX1 deficiency. Western blot analysis confirmed lack of HMOX1 protein upon oxidant stimulation of the patient cells.

Conclusions Here, we describe a phenotype expansion for HMOX1-deficiency to include not only asplenia and hepatomegaly, but also interstitial lung disease with cholesterol granulomas and inflammatory flares with hemophagocytosis present in the bone marrow.

Background

Heme oxygenases are rate-limiting enzymes that catalyze the degradation of heme to carbon monoxide (CO), ferrous iron, and biliverdin, which then becomes bilirubin via the action of biliverdin reductase. Two isoforms exist, heme oxygenase-1 (HMOX1) and heme oxygenase-2 (HMOX2), with CO, biliverdin, and bilirubin implicated in important cellular processes, such as inflammation, cell proliferation, apoptosis, and antioxidant defense. HMOX1 is distributed in the liver, spleen, and endothelium with rapid induction in the presence of stressors, while HMOX2 expression is widespread and cannot be induced. HMOX1 was first discovered in the 1968 (1) but the first case of HMOX1 deficiency was not described until 1999 (2).

HMOX1 deficiency is an extremely rare autosomal recessive disorder with only four other cases reported to date (2-6). The rarity may derive from the role of fetal HMOX1 in placental health (7, 8). Clinical presentation is complex and diverse, including direct antibody negative hemolytic anemia, low bilirubin, and hyperinflammation (3). HMOX1 is induced in the liver, spleen and endothelium after oxidative stressors and hypoxia (3). One reported case appeared to mimic vasculitis and another was thought to have hemophagocytic lymphohistiocytosis (HLH). Diagnosis of HMOX1 deficiency lies within clinical findings and laboratory studies with genetic testing of *HMOX1* required for confirmation.

Here, we describe a boy born to nonconsanguineous parents who presented with early onset asplenia, recurrent infections, and associated flares with bone marrow histiocyte activation with worsening interstitial lung disease.

Results

Clinical examination

A 10-year-old boy was admitted for diagnostic lung biopsy in the setting of progressive chronic hypoxic respiratory failure and recurrent hyperinflammatory episodes. He was born at 7 pounds 3 ounces at estimated gestational age of 36 weeks via normal spontaneous vaginal delivery to a mother with a history of placental clots with a still birth at term. He was hospitalized at 4 months of age for respiratory syncytial virus (RSV) for 7 days, at 1 year old for hypospadias repair, and then again at age 3 years 8 months for what was thought to be mononucleosis due to positive Epstein-Barr virus (EBV) positive immunoglobulin M (IgM). During the latter episode, he was severely fatigued and had persistent fevers to 40 °C. Additionally, he had another RSV infection at 3 years and 4 months of age. He demonstrated mild gross motor developmental delay as he did not crawl and did not walk until 19 months of age. He was also fully vaccinated until 3 years of age.

At approximately 4 years of age, he presented with a one-month history of fatigue, intermittent fevers and dark urine. His fevers were daily reaching 40 °C with periods of defervescence. He then developed a cough with hypoxemia to 89% on room air and was admitted for viral bronchiolitis. Physical exam was notable for mild prognathism, slight frontal bossing, low-set and posteriorly rotated ears, mild pectus excavatum, bilateral undescended testes, and long fingers and toes with overlapping second and fourth toes over the third toes bilaterally were noted. His elbows and knees were hyperextensible and demonstrated moderate pes planus and out-toeing.

During hospitalization, hepatomegaly was found along with mild transaminitis (AST 301 U/L, ALT 74 U/L), direct antiglobulin test negative hemolytic anemia (hematocrit 24.7%) and hemoglobinuria without microscopic red blood cells. Abdominal CT scan revealed a small poorly perfused spleen which correlated well with the Howell-Jolly bodies and schistocytes on peripheral smear. Bilirubin was normal but lactate dehydrogenase (LDH) was dramatically elevated at 19,706 U/L. Normal renal function was present with creatinine 0.1 mg/d without evidence of proteinuria or myoglobinuria. Creatine kinase values were normal at 202 IU/L. Systemic inflammation was present with leukocytosis (peak 53.8 K/mm³), thrombocytosis (peak 914 k/mm³), elevated erythrocyte sedimentation rate (ESR, 87 mm/hr), hyperferritinemia to 1,980 ng/mL, but blood cultures and respiratory viral PCR panel was negative.

He had a liver biopsy that demonstrated mild sinusoidal fibrosis, mild microvesicular steatosis, and rare apoptotic hepatocytes, but ultimately was non-diagnostic. Work up for hypercoagulability, serum muscle enzymes and amino acid and organic acids from the urine and plasma were all normal. Serologies for antiphospholipid antibody syndrome, antineutrophil cytoplasmic antibodies, anti-nuclear antibody, anti

RNP, and anti-SSA/SSB were all negative. Autoimmune hepatitis work-up yielded negative liver kidney microsomal and smooth muscle antibodies. Respiratory symptoms slowly resolved and hematologic findings improved, thus representing a flare that recurred regularly over the next 6 years.

During his next flare, the patient had anemia, leukocytosis, and thrombocytosis along with abdominal pain, hepatomegaly, and fevers. Further imaging with CTA abdomen demonstrated absent splenic veins and multiple collaterals to a small left kidney, implying that patient's spleen had infarcted. A bone marrow biopsy demonstrated extensive histiocyte activation with phagocytosis of nucleated red blood cell precursors. There was normal cellularity but decreased trilineage hematopoiesis and increased megakaryocytes; no malignant cells were present. This flare was associated with HHV-7 viremia.

He was readmitted to the hospital multiple times for similar febrile episodes found to be triggered by viral and bacterial infections as well as Prevnar vaccination (Fig. 1). He had a prolonged four-month long flare following H1N1 infection complicated by pneumonia with pleural effusion. He received the Prevnar 13 vaccination and developed another hyperinflammatory episode lasting four months complicated by steroid responsive pericardial effusion and presumed inflammatory pneumonitis. He soon became oral corticosteroid-dependent as weaning resulted in hemolysis and dark urine. By the age of 8, the flares were characterized less by persistent febrile episodes but more by shortness of breath, chest discomfort and intermittent desaturations. His growth curve had started to plateau at age 4 despite being at the 50th percentile until the age of 3; he was less than the 10th percentile for weight and 20th percentile for height. He also began experiencing hip pain with unequal leg lengths, difficulty running, and decreased stamina. Mild knee swelling was noted accompanying myalgias and arthralgias with morning stiffness. Mild proteinuria developed as well. He was steroid responsive and therefore treated with oral prednisone 10 mg twice daily. Steroid sparing therapies, such as methotrexate and azathioprine, were introduced by discontinued because no benefit was observed.

Due to persistent and progressive respiratory symptoms exacerbated by an infection with RSV and mycoplasma, he was hospitalized at Seattle Children's Hospital for further evaluation. Spirometry testing demonstrated a severely restrictive pulmonary pattern with a forced vital capacity (FVC) of 0.41 L (20%), forced expiratory volume in 1 second (FEV1) of 0.41 (22%), and FEV1/FVC 99%. He underwent a right thoracoscopic lung biopsy, which demonstrated extensive fibrotic nonspecific interstitial pneumonia (NSIP), patchy pleural fibrosis, and scattered cholesterol granulomas.

Following the procedure, he developed a right hemothorax and pneumothorax with respiratory distress and supplemental oxygen, requiring Pediatric Intensive Care Unit (PICU) admission. He had substantial fibrotic intrathoracic tissue and his pulmonary function continued to deteriorate, requiring consistent use of nasal cannula and increased use of BiPAP. In an attempt to treat his inflammatory state, corticosteroid dose was increased and gradually weaned while anti-IL-1R therapy (anakinra), was trialed for 10 days, overlapping with cyclosporine, and then switched to anti-IL-6 therapy (tocilizumab) with minimal benefit. He expired just prior to his eleventh birthday due to respiratory failure.

Patient Laboratory, Histopathology, and Radiologic Evaluation

During episodes, his baseline leukocytosis increased from about 20 K/mm³ to exceed 40 K/mm³. Hyposplenism, initially noted at age 4, was confirmed on serial abdominal imaging, contributed to baseline thrombocytosis, but platelet counts exceeded 1 million frequently during flares, requiring aspirin for coagulation prophylaxis. At baseline, he had mild anemia with hematocrit of high 30%/low 40s%. However, during flares, his hematocrit would nadir below 30%. LDH was elevated at baseline and episodically reached 28,000 U/L with uniformly elevated isoenzymes. His transaminitis largely remained within the mild range with corresponding mild elevation of GGT and INR (Table 1). Alpha-1 antitrypsin was normal at 245 mg/dL as was alpha fetoprotein (0.9 ng/mL). Metabolic etiologies were ruled out with plasma and urine amino acid levels as well as urine organic acid levels.

Table 1

Laboratory studies. ALT – alanine aminotransferase, AST – aspartate aminotransferase, CH50 – total hemolytic complement activity, GGT – γ -glutamyl transferase, HDL – high density lipoprotein, IgA – immunoglobulin A, IgD – immunoglobulin D, IgG – immunoglobulin G, IgM – immunoglobulin M, INR – international normalized ratio, LDH – lactate dehydrogenase, LDL – low density lipoprotein, NK – natural killer cell, PHA – phytohemagglutinin, PPSV23 – pneumococcal vaccine polyvalent, sIL-2R – soluble interleukin-2 receptor.

Test	Normal Values	Patient's Values	Test	Normal Values	Patient's Values
Biochemical			Immunological		
ALT	5–41 IU/L	165–615	IgG	608–1572 mg/dL	1050–1140
AST	6–40 IU/L	44–157	IgA	52–242 mg/dL	262
GGT	15–85 IU/L	30–405	IgM	45–236 mg/dL	89–108
Total bilirubin	0.0–1.1 mg/dL	0.2	IgE	0.98–570.6 mg/dL	105
INR	< 1.0	1.2–1.6	IgD	≤ 10 mg/dL	3
Fibrinogen	230–450 mg/dL	57–493	PPSV23	$\geq 8/21$ ($\geq 5/12$)	8/21 (5/12)
D-dimer	≤ 0.5 mg FEU/mL	> 20	Tetanus	≥ 0.01 IU/mL	0.43
Ceruloplasmin	29–56 mg/dL	48	C3	83–203 mg/dL	186
Liver copper	10–35 μ g/g dry weight	43	C4	16–52 mg/dL	24
Plasma copper	56–191 mcg/dL	191	CH50	> 32 unit/mL	69
Triglycerides	60–135 mg/dL	95–503	CD3	1,200–2,600/mm ³	1465
LDL	< 110 mg/dL	324	CD4	650–1,500/mm ³	3793
HDL	> 39 mg/dL	58	CD8	370–1,100/mm ³	2117
Total LDH	145–345 U/L	5490–28,019	CD4:CD8	> 2:1	1.8:1

Test	Normal Values	Patient's Values	Test	Normal Values	Patient's Values
LDH 1 (%)	17.5–28.3% (I, Heart)	7.5–10	CD16 ⁺ CD56 ⁺	120–480/mm ³	882
LDH 2 (%)	30.4–36.4% (II)	17.6–21	CD19	270–860/mm ³	1588
LDH 3 (%)	19.2–24.8% (III)	26.9	PHA	> 30%	24.70%
LDH 4 (%)	9.6–15.6% (IV)	23.7	anti-CD3	> 30%	21.50%
LDH 5 (%)	5.5–12.7% (V, Liver)	24.3	NK function		
Ferritin	10–300 ng/mL	555–4264	50:1	> 20	11
sIL-2R	45-1105 U/mL	145	25:1	> 10	9
			12.5:1	> 5	5
			6.25:1	> 1	5
			Lytic units	> 3.1	2.5

During two separate hospitalizations for flares, the diagnosis of hemophagocytic lymphohistiocytosis (HLH) and macrophage activation syndrome (MAS) were both considered based upon his laboratory features. Overall, two bone marrow biopsies were performed approximately one year apart and both demonstrated normal cellularity and markedly increased hemophagocytosis (Fig. 2). Natural killer (NK) cell function was assessed and was decreased (Table 1). CD107a could not be assessed due to insufficient NK cells. Soluble IL-2 receptor (sIL-2R, also known as soluble CD25) was normal and never elevated. Genetic testing for periodic fever syndromes and familial HLH were performed, but pathogenic variants in known genes were identified. Comparative genomic hybridization (CGH) revealed no structural variants, and he had a normal male karyotype.

Given his recurrent infections, an immune evaluation was performed revealing abnormal T cell proliferation to stimulation with both phytohemagglutinin (PHA) and anti-CD3 (Table 1). He had increased naïve CD45RA⁺CD27⁺CCR7⁺ population (65% of cells), few effector memory T cells, and likewise immature CD8⁺ population with > 65% of the cells naïve. He had normal quantitative immunoglobulin levels and robust vaccine responses, but B cell immunophenotyping was notable for absent immature and transitional B cells with reduced CD27⁺ memory B at 6% (normal > 8%). Class switched and BAFF receptor populations were normal. Further T cell analysis was not performed.

Genetic analysis

Whole exome sequencing of patient, mother, father, and brother were performed revealing a compound heterozygous paternal frame shift a paternal frame shift HMOX1 c.264delCTGG (p.L89Sfs*24) and maternal splice donor HMOX1 (c.636 + 2 T > A) consistent with HMOX1 deficiency. Western blot analysis subsequently confirmed that cells treated with a known inducer of HMOX1, Cobalt protoporphyrin (CoPP), resulted in no protein was expressed (Fig. 3), confirming HMOX1 deficiency.

Discussion

The boy reported herein is the fifth individual reported with HMOX1 deficiency and is notable for the presence of unique clinical findings due to chronic pulmonary disease. He was found on thorascopic lung biopsy to have extensive interstitial fibrosis, consistent with the fibrotic nonspecific interstitial pneumonia (NSIP) pattern, in addition to cholesterol granulomas. NSIP is a diffuse lung disease that may have a cellular, fibrotic, or mixed pattern. It is the most common of the diffuse lung diseases in the pediatric population often associated with a systemic disease. The majority of diffuse lung diseases are attributed to defects in surfactant dysfunction or connective tissue diseases, such as systemic lupus erythematosus, polymyositis/dermatomyositis, systemic sclerosis, mixed connective tissue disease, and systemic juvenile idiopathic arthritis (9, 10). Surfactant disorders account for many interstitial lung disease cases in both pediatrics and adults previously thought to be idiopathic (11).

Cholesterol granulomas are also rare, especially in children. Pulmonary interstitial and intra-alveolar cholesterol granulomas (PICG) are formed when degenerating macrophages release cholesterol esters in the interstitium and with organization form granulomas. The cholesterol appears as acicular crystals on light microscopy (Fig. 2). PICG typically appears in the setting of lipoid pneumonia with or without pulmonary alveolar proteinosis (12). Exogenous lipoid pneumonia results from inhalation or aspiration of mineral, plant or animal-based oils, and/or ascending aspiration of such oils in the setting of gastroesophageal reflux (13, 14). In this case, there was no history suggestive of exogenous oil aspiration or gastroesophageal reflux. However, PICGs due to endogenous etiologies without lipoid pneumonia are very rare and has been reported in pulmonary hypertension (15, 16) or in the setting of systemic juvenile idiopathic arthritis (sJIA) (17).

Our patient developed severe NSIP, likely due to oxidant-induced injury (18), which has not been reported in other patients with HMOX1 deficiency. In a post-mortem analysis of one patient, there were microthrombi in the arterioles and capillaries of the lungs with focal alveolitis, but no chronic lung changes. In another case, there was diffuse alveolar hemorrhage reported with suspicion of small vessel vasculitis and yet another case reported HMOX1 deficiency as a mimic of childhood vasculitis outside the lungs (5). Although oxidant-induced lung injury has been discussed in murine models of HMOX1 deficiency, previously reported patients did not develop pulmonary complications prior to their death. The pulmonary features in our case showed progressive fibrosis and cholesterol granulomas that may be related to the macrophage activation as similar histology has been reported in sJIA. Another case of HMOX1 has been reported as a mimic of HLH (6). Absent NK cell function was observed in the setting of

persistent fevers, hypertriglyceridemia, hyperferritinemia, and elevated sIL-2R, and a diagnosis of HLH. Immune evaluations were not performed in prior patients with HMOX1 deficiency.

During flares, our patient had features of HLH including hepatomegaly, hemophagocytosis in the bone marrow, absent NK cell functional activity, and hyperferritinemia. Genetic HLH panel testing was sent but no pathogenic variants were identified. Hemophagocytosis can also be seen secondary to underlying rheumatologic conditions termed macrophage activation syndrome (MAS), a rare and potentially fatal disorder, thought to result from uncontrolled activation and proliferation of T cells and excessive activation of macrophages. The most common etiology of MAS is sJIA, a diagnosis of exclusion (19).

The lung biopsy of our patient and presence of hemophagocytes in the bone marrow were consistent with sJIA (20), but our patient lacked many clinical and laboratory features of MAS during his flares. The consensus MAS Study Group (21) identified key features, including down-trending platelets, hyperferritinemia (although typically higher than the 500 ng/mL cutoff set in the HLH-2004 criteria (22)), falling leukocyte count and ESR, hypofibrinogenemia and persistent continuous fevers (≥ 38 °C), all of which our patient lacked. Elevated sIL-2R, triglycerides, LDH, and transaminases can also be found elevated in MAS, although these can be nonspecific.

Hemophagocytosis can also be observed acutely in infection and malignancy, although the chronicity of his condition and extensive malignancy work-up made these conditions less likely. Lastly, rare inborn errors of metabolism have also been rarely associated with hemophagocytosis, including lysosomal storage disorders such as Gaucher disease (23), organic acidemia (24), or Wolman disease (25). As such, screening and genetic tests for lysosomal enzyme function, fibroblast cultures, and urine mucopolysaccharides and oligosaccharides were performed in our patient but were normal.

HMOX1 deficiency results in overt heme concentrations, low bilirubin, and marked oxidative stress with varied phenotype rooted in hemolytic anemia, low bilirubin, and hyperinflammation. TLR9 in mice has been found to induce HMOX1 expression in bone marrow dendritic cells, which in turn regulates macrophage production of IL-10 that is highly involved in MAS when dysregulated (26). Furthermore, the defect in HMOX1 putatively impairs phagocytosis (3) with a murine study demonstrating subablative bone marrow transplantation of HMOX1 deficient mice reverses disease due to repopulation of wild type macrophages (27). Therefore, while speculative, myeloablative bone marrow transplantation may be a treatment option for these children with HMOX1 deficiency.

Conclusions

We report a young man with HMOX1 deficiency that illustrates that patients with HMOX1 deficiency may appear to have autoimmune disease, such as sJIA, systemic lupus erythematosus, or vasculitis due to a picture of NSIP combined with PICG and presence of surfactant by immunostaining in the setting of daily fevers, arthritis of knees and right ankle, leukocytosis, thrombocytosis, anemia, elevated inflammatory markers, and hyperferritinemia. Laboratory evaluation, possible arthritis, and lung pathology in our patient mimicked longstanding sJIA with MAS and interstitial lung disease. However, our patient did not

fully meet diagnostic criteria for sJIA and MAS. In previously reported patients, presentations have been variable, but have notably included hemolytic anemia, normal bilirubin, hyperinflammation, and asplenia in the setting of features strongly suggestive of autoimmune disease. We highlight that patients with HMOX1 deficiency can also have marked lung disease that can result in early mortality.

Methods

Subjects. Subjects were consented into the Genetic Basis of Immunodeficiency Diseases Biorepository at the Seattle Children's Hospital (IRB #11738) and also consented for the University of Washington Repository for Mendelian Disorders for genetic studies approved by the University of Washington Institute Review Board all in compliance with consent for deposition into the database of Genotypes and Phenotypes (dbGaP).

Whole exome sequencing. Whole exome sequencing was performed in collaboration with University of Washington Center for Mendelian Genomics (UWCMG) on our quad family with one affected proband, unaffected brother, father and mother. In brief, 1 mg genomic DNA was subjected to a series of shotgun library construction steps, including fragmentation through acoustic sonication (Covaris), end-polishing (NEBNext End Repair Module), A-tailing (NEBNext dA-Tailing Module) and ligation of 8 bp barcoded sequencing adaptors (Enzymatics Ultrapure T4 Ligase). Prior to exome capture, the library was PCR amplified (BioRad iProof). We hybridized 1 mg barcoded shotgun library to capture probes targeting 64 Mb of coding exons (Roche Nimblegen SeqCap EZ Human Exome Library v.3.0) per the manufacturer's protocol, except that we added custom blockers complementary to the full length of the flanking adaptor and barcodes. Enriched libraries were amplified by PCR before sequencing was performed (BioRad iProof). Library quality was determined from molecular-weight distribution and sample concentration (Agilent Bioanalyzer). Pooled, barcoded libraries were sequenced via paired-end 50 bp reads with an 8 bp barcode read on Illumina HiSeq sequencers. Demultiplexed BAM files were aligned to a human reference (hg19) with the Burrows-Wheeler Aligner (0.6.1). All aligned read data were subjected to (1) removal of duplicate reads (Picard), (2) indel realignment with the GATK IndelRealigner, and (3) base quality recalibration with GATK Recalibration. Variant detection and genotyping were performed with the UnifiedGenotyper (UG) tool from GATK (refv1.6). Variant data for each sample were formatted as a variant call format (v.4.0) and flagged with the filtration walker (GATK) to mark sites that were of lower quality and were potential false positives (e.g., they had quality scores ≤ 50 , allelic imbalance $R \leq 0.75$, long homopolymer runs (> 3), and/or low quality by depth (QD) < 5). PLINKv 1.90b2m was used to verify sex of each individual. Pedigree relationships were verified against the results from KINGv1.4.0 software (kinship between parents = 0.0078). Ancestry was checked with PRIMUS using principal components analysis (PCA) and the family cluster with members of the HAPMAP population "Gujarati Indians from Houston". Variants were annotated with Variant Effect Predictor (VEP) v83 and then analyzed using GEMINI v0.18 (Paila U, Chapman BA, Kirchner R, Quinlan AR (2013) GEMINI: Integrative Exploration of Genetic Variation and Genome Annotations. PLoS Comput Biol 9(7): e1003153.

doi:10.1371/journal.pcbi.1003153). Analysis used the compound heterozygous query and excluded variants present at high frequency in the 1000 Genomes, EXAC browser or the Exome Sequencing Project

(ESP) data. Low quality or potential false positives (quality scores ≥ 30 , long homopolymer runs > 5 , low quality by depth < 5 , within a cluster of SNPs). Sanger sequencing also confirmed the variants.

Western Blot. Primary peripheral blood mononuclear cells were cultured overnight in complete RPMI media supplemented with 10% fetal calf serum prior to incubating with 10 μ M Cobaltic Protoporphyrin IX Chloride (Santa Cruz Biotechnologies #sc-294098, Santa Cruz, CA) for 24 hours. Cells were lysed in RIPA lysis buffer (Thermo Fisher #89900) and run on NuPAGE 4-12% gradient Bis-Tris Protein gels (Thermo #NP0322) and transferred to nitrocellulose using iBlot2 transfer device. Membranes were blocked using Odyssey Blocking Buffer (LiCor #927-40000) and stained using anti-Human/Mouse HO-1/HMOX1 (R&D #MAB3776)[Monoclonal Rat IgG_{2B} Clone # 412811] at 1:1000 dilution and detected using Odyssey anti-rat IgG (H+L) IRDye 800CW secondary reagent (1:15,000).

Abbreviations

ALT: Alanine transaminase; AST: Aspartate transaminase; BMbx: Bone marrow biopsy; bx: Biopsy, CGH: Comparative genomic hybridization (CGH); CH50: Total hemolytic complement activity; CoPP: Cobalt protoporphyrin; EBV: Epstein Barr virus; ESR: Erythrocyte sedimentation rate; FEV1: forced expiratory volume in 1 second; FVC: Forced vital capacity; HMOX1: Heme oxygenase-1; HLH: Hemophagocytic lymphohistiocytosis; GGT: γ -glutamyl transferase; HDL: High density lipoprotein; IgA: Immunoglobulin A; IgD: Immunoglobulin D; IgG: Immunoglobulin G; IgM: Immunoglobulin M; INR: International normalized ratio; LDH: Lactate dehydrogenase; LDL: Low density lipoprotein; MAS: Macrophage activation syndrome; NK: Natural killer; NSIP: Nonspecific interstitial pneumonia; NSVD: Normal spontaneous vaginal delivery; PHA: phytohemagglutinin; PICG: Pulmonary interstitial and intra-alveolar cholesterol granulomas; PNA: Pneumonia; Pnevna 13: Pneumococcal 13-valent conjugate vaccine (diphtheria CRM197 protein); PPSV23: Pneumococcal vaccine polyvalent; RSV: Respiratory syncytial virus; R: Right; RML: Right middle lobe; RSV: Respiratory syncytial virus; sIL-2R: Soluble interleukin-2 receptor; sJIA: systemic juvenile idiopathic arthritis; URI: Upper respiratory infection; VATS: Video-assisted thorascopic surgery.

Declarations

Ethics approval and consent to participate

The study was approved by the Institutional Review Board of Seattle Children's Hospital and separately approved by the University of Washington Human Subjects Review Committee.

Consent for publication

Obtained with research protocol for Seattle Children's Hospital Immunology Biorepository.

Availability of data and materials

Not applicable.

Competing interests

The authors declare that they have no competing interests

Funding

Sequencing was provided by the University of Washington Center for Mendelian Genomics (UW-CMG) and was funded by NHGRI and NHLBI grants UM1 HG006493 and U24 HG008956. The content is solely the responsibility of the authors and does not necessarily represent the official views of the National Institutes of Health.

Authors' contributions

ASC was a major contributor to writing and revising the manuscript. BC performed the histological examination of the pulmonary, hepatic, and bone marrow tissue. JB analyzed and interpreted the patient data regarding the pulmonary disease. KN and TRT contributed to patient assessments and interpretation of clinical data. ABIR performed Western blot analysis. MJB and DAH supervised the genetic analysis and contributed to the manuscript. EJA performed the genetic sequencing, analysis, contributed to the assessment of the patient, and supervised the drafting and finalizing of the manuscript. All authors read and approved the final manuscript.

Acknowledgements

We would like to acknowledge Tara Bumgarner for helping with IRB submissions and Josh Smith for help in learning the genomic analysis pipeline.

References

1. Tenhunen R, Marver HS, Schmid R. The enzymatic conversion of heme to bilirubin by microsomal heme oxygenase. *Proceedings of the National Academy of Sciences of the United States of America*. 1968;61(2):748-55.
2. Yachie A, Niida Y, Wada T, Igarashi N, Kaneda H, Toma T, et al. Oxidative stress causes enhanced endothelial cell injury in human heme oxygenase-1 deficiency. *The Journal of clinical investigation*. 1999;103(1):129-35.
3. Kawashima A, Oda Y, Yachie A, Koizumi S, Nakanishi I. Heme oxygenase-1 deficiency: the first autopsy case. *Human pathology*. 2002;33(1):125-30.
4. Radhakrishnan N, Yadav SP, Sachdeva A, Pruthi PK, Sawhney S, Piplani T, et al. Human heme oxygenase-1 deficiency presenting with hemolysis, nephritis, and asplenia. *Journal of pediatric hematology/oncology*. 2011;33(1):74-8.

5. Gupta A, Akihiro Y, Saxena AK, Bhattacharya A, Singh S. Haem oxygenase-1 deficiency: a mimicker of childhood vasculitis. *Scandinavian journal of rheumatology*. 2016;45(2):165-6.
6. Greil J, Verga-Falzacappa MV, Echner NE, Behnisch W, Bandapalli OR, Pechanska P, et al. Mutating heme oxygenase-1 into a peroxidase causes a defect in bilirubin synthesis associated with microcytic anemia and severe hyperinflammation. *Haematologica*. 2016;101(11):e436-e9.
7. Ozen M, Zhao H, Lewis DB, Wong RJ, Stevenson DK. Heme oxygenase and the immune system in normal and pathological pregnancies. *Front Pharmacol*. 2015;6:84.
8. Tsur A, Kalish F, Burgess J, Nayak NR, Zhao H, Casey KM, et al. Pravastatin improves fetal survival in mice with a partial deficiency of heme oxygenase-1. *Placenta*. 2019;75:1-8.
9. Fan LL, Dishop MK, Galambos C, Askin FB, White FV, Langston C, et al. Diffuse Lung Disease in Biopsied Children 2 to 18 Years of Age. Application of the chILD Classification Scheme. *Ann Am Thorac Soc*. 2015;12(10):1498-505.
10. Cottin V, Hirani NA, Hotchkiss DL, Nambiar AM, Ogura T, Otaola M, et al. Presentation, diagnosis and clinical course of the spectrum of progressive-fibrosing interstitial lung diseases. *Eur Respir Rev*. 2018;27(150).
11. Nathan N, Borensztajn K, Clement A. Genetic causes and clinical management of pediatric interstitial lung diseases. *Curr Opin Pulm Med*. 2018;24(3):253-9.
12. Fisher M, Roggli V, Merten D, Mulvihill D, Spock A. Coexisting endogenous lipid pneumonia, cholesterol granulomas, and pulmonary alveolar proteinosis in a pediatric population: a clinical, radiographic, and pathologic correlation. *Pediatr Pathol*. 1992;12(3):365-83.
13. Marangu D, Gray D, Vanker A, Zampoli M. Exogenous lipid pneumonia in children: A systematic review. *Paediatr Respir Rev*. 2019.
14. Hu X, Lee JS, Pianosi PT, Ryu JH. Aspiration-related pulmonary syndromes. *Chest*. 2015;147(3):815-23.
15. Glancy DL, Frazier PD, Roberts WC. Pulmonary parenchymal cholesterol-ester granulomas in patients with pulmonary hypertension. *The American journal of medicine*. 1968;45(2):198-210.
16. Fischer EG, Marek JM, Morris A, Nashelsky MB. Cholesterol granulomas of the lungs associated with microangiopathic hemolytic anemia and thrombocytopenia in pulmonary hypertension. *Arch Pathol Lab Med*. 2000;124(12):1813-5.
17. Schultz R, Mattila J, Gappa M, Verronen P. Development of progressive pulmonary interstitial and intra-alveolar cholesterol granulomas (PICG) associated with therapy-resistant chronic systemic juvenile arthritis (CJA). *Pediatr Pulmonol*. 2001;32(5):397-402.
18. Choi AM, Alam J. Heme oxygenase-1: function, regulation, and implication of a novel stress-inducible protein in oxidant-induced lung injury. *American journal of respiratory cell and molecular biology*. 1996;15(1):9-19.
19. Minoia F, Davi S, Horne A, Demirkaya E, Bovis F, Li C, et al. Clinical features, treatment, and outcome of macrophage activation syndrome complicating systemic juvenile idiopathic arthritis: a multinational, multicenter study of 362 patients. *Arthritis Rheumatol*. 2014;66(11):3160-9.

20. Saper VE, Chen G, Deutsch GH, Guillerman RP, Birgmeier J, Jagadeesh K, et al. Emergent high fatality lung disease in systemic juvenile idiopathic arthritis. *Ann Rheum Dis*. 2019; 78:1722-31.
21. Davi S, Consolaro A, Guseinova D, Pistorio A, Ruperto N, Martini A, et al. An international consensus survey of diagnostic criteria for macrophage activation syndrome in systemic juvenile idiopathic arthritis. *J Rheumatol*. 2011;38(4):764-8.
22. Henter JI, Horne A, Arico M, Egeler RM, Filipovich AH, Imashuku S, et al. HLH-2004: Diagnostic and therapeutic guidelines for hemophagocytic lymphohistiocytosis. *Pediatr Blood Cancer*. 2007;48(2):124-31.
23. Sharpe LR, Ancliff P, Amrolia P, Gilmour KC, Vellodi A. Type II Gaucher disease manifesting as haemophagocytic lymphohistiocytosis. *J Inherit Metab Dis*. 2009;32 Suppl 1:S107-10.
24. Gokce M, Unal O, Hismi B, Gumruk F, Coskun T, Balta G, et al. Secondary hemophagocytosis in 3 patients with organic acidemia involving propionate metabolism. *Pediatric hematology and oncology*. 2012;29(1):92-8.
25. Taurisano R, Maiorana A, De Benedetti F, Dionisi-Vici C, Boldrini R, Deodato F. Wolman disease associated with hemophagocytic lymphohistiocytosis: attempts for an explanation. *Eur J Pediatr*. 2014;173(10):1391-4.
26. C B, T B, N C, E B. Monomethyl Fumarate as a Novel Therapy for Macrophage Activation Syndrome: Mechanism of Action in an Animal Model [abstract]. *Arthritis Rheumatol*. 2019;71.
27. Kovtunovych G, Ghosh MC, Ollivierre W, Weitzel RP, Eckhaus MA, Tisdale JF, et al. Wild-type macrophages reverse disease in heme oxygenase 1-deficient mice. *Blood*. 2014;124(9):1522-30.

Figures

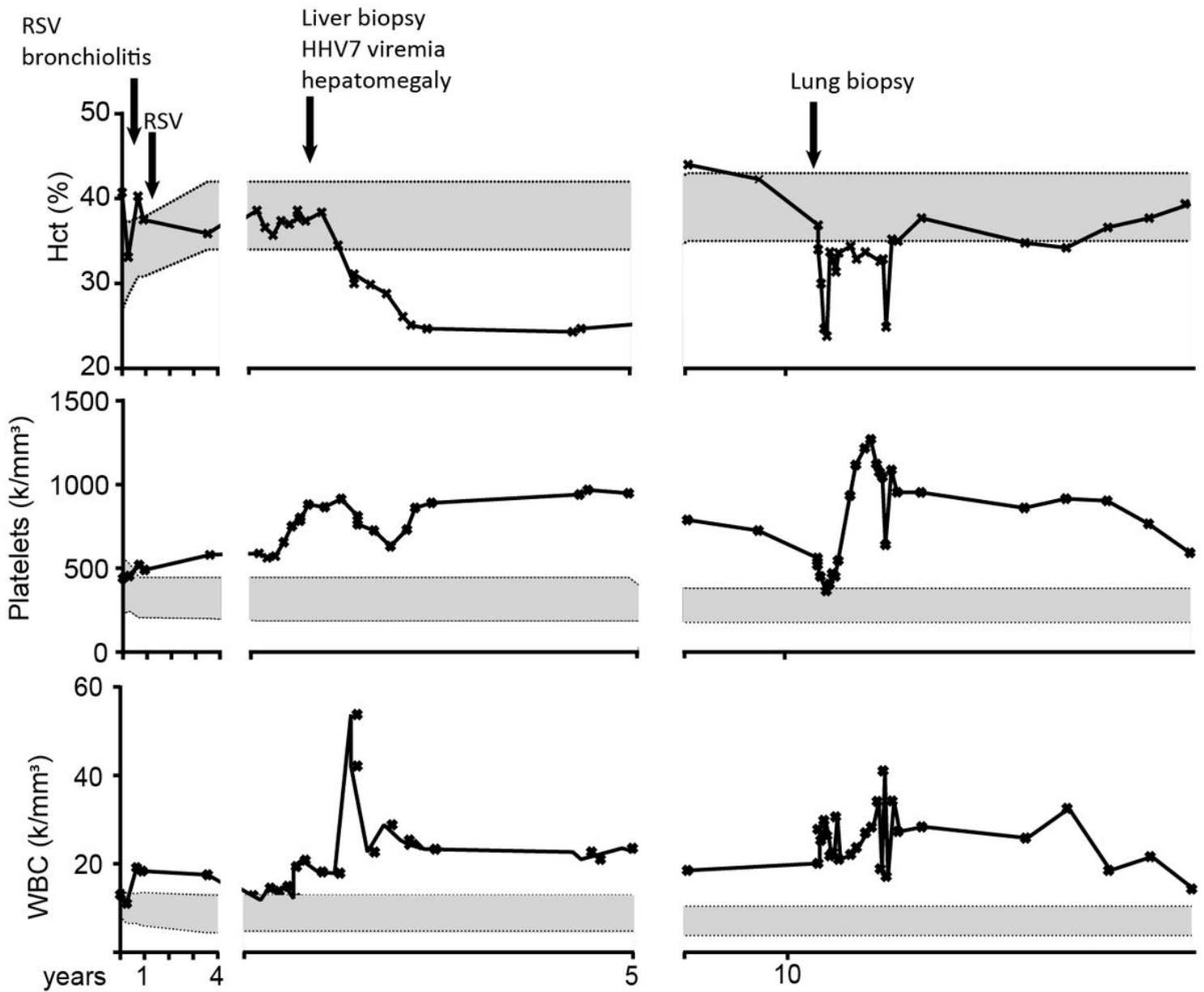


Figure 1

Clinical course. Trends of patient's laboratory values for white blood count (WBC), platelets (Plts), and hematocrit (Hct) at baseline and during known flares (arrows). Note that patient's overall baseline and flare values progressively became more abnormal as he aged with leukocytosis and thrombocytosis becoming increased and anemia becoming more pronounced. Normal age-matched ranges denoted with grey shading.

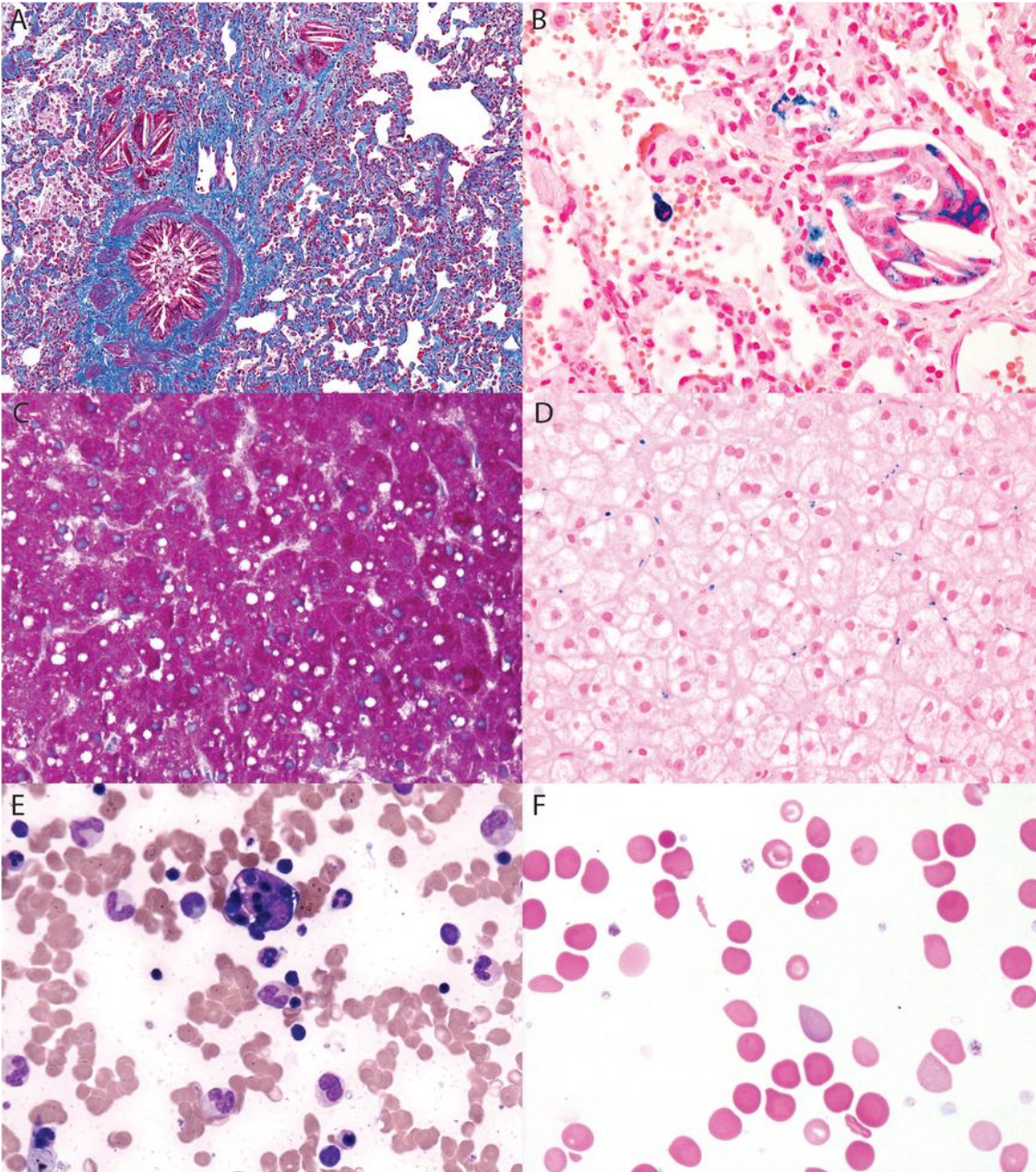


Figure 2

Histopathology. (A) Trichrome stained sections from lung biopsy tissue demonstrate extensive alveolar septal fibrosis and scattered granulomas. (B) Iron staining of lung tissue highlights hemosiderin laden macrophages (blue granules) associated with cholesterol granulomas. (C) Trichrome stained liver biopsy with mild sinusoidal fibrosis and microvesicular steatosis and (D) iron stained liver biopsy with increased iron (blue granules) in Kupffer cells (blue). (E) Wright stained bone marrow aspirate

demonstrating hemophagocytosis. (F) Peripheral blood smear demonstrating anisocytosis, schistocytes, elliptocytes, and a Howell-Jolly body.

Figure 3.

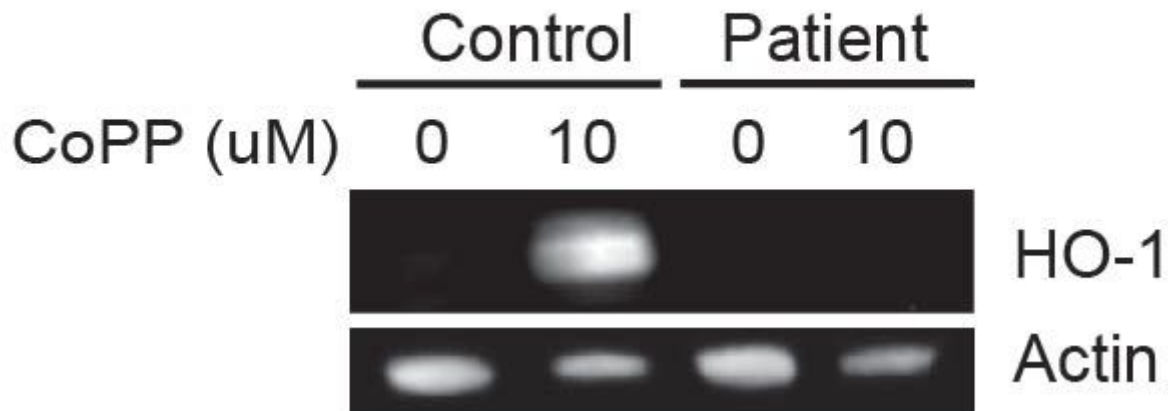


Figure 3

HMOX1 expression. Western blot analysis of HMOX1 following induction with cobalt protoporphyrin (CoPP) for 24 hours of patient's peripheral blood mononuclear cells compared to control cells. Patient is demonstrated to lack expression of HMOX1.